



International Atomic Energy Agency

Application of Tomography methods in EAST Line-Integrated Radiation Diagnostics

L. Q. Xu¹, Y. M. Duan¹, Y. Chao^{1,2}, C.W. Mai^{1,2}, K.Y.Chen¹, E.Z.Li¹,
H.X.Qu^{1,2}, S.Y.Lin¹, T.B.Wang³ and L. Q. Hu¹

¹Institute of Plasma Physics, Chinese Academy of Sciences, Hefei 230031, China

²University of Science and Technology of China, Hefei 230026, China

³Southwestern Institute for Physics, CNNC, Chengdu 610200, China

30th Nov – 3th Dec 2021

Topical issues on Inverse Problem

4th IAEA Technical Meeting on Fusion Data Processing, Validation and Analysis

Outline

I. 2-D tomographic reconstruction

II. Tomography methods on EAST

- Abel method
- Fourier-Bessel method (SXR)
- Constrained optimization method (divertor XUV)
- L-curve Tikhonov method (GEM)
- Gaussian progress method (SXR, HX and XUV)
- Neural network method (CNN, FCNN and VGGNet)

III. Applications

- MHD mode structure analysis (by SVD)
- Impurity density estimation

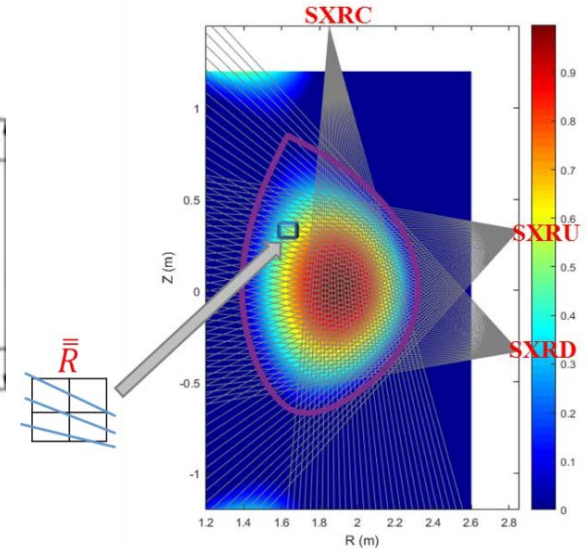
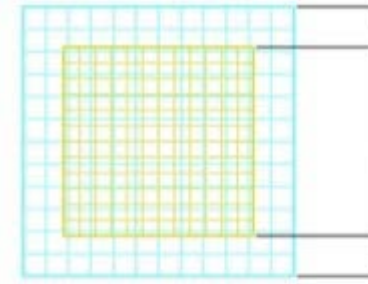
IV. Summary and Outlook



2-D tomographic reconstruction

- **Line-Integrated diagnostics**

- Soft X-ray
- XUV/bolometer
- Gas Electron Multiplier
- Hard X-ray
- Point
- EUV, XCS...

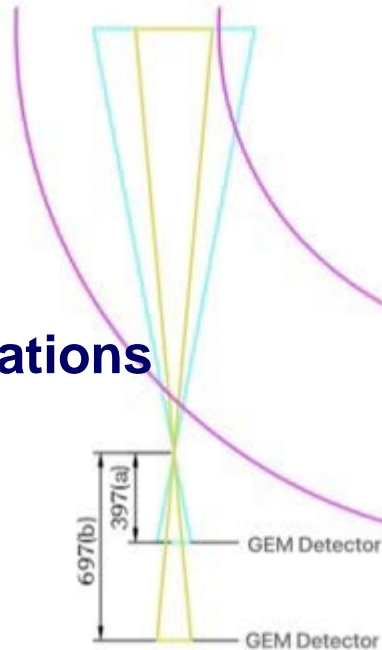


LOS of SXR system

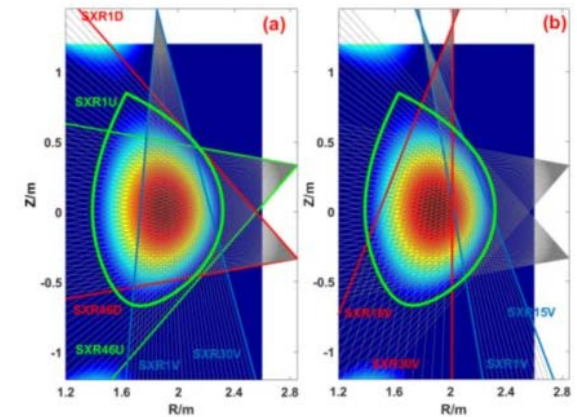
- **Forward model**

- More unknowns than equations
- ill-posed problem

$$\bar{d}_M = \bar{R} \bar{E}_N$$



GEM Tangential camera



LOS of XUV system



Forward and inverse problems

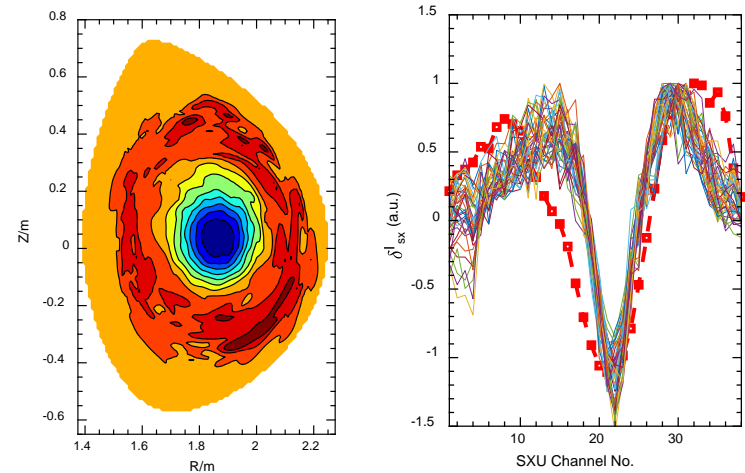
- **Forward problem**

- From \bar{E}_N to \bar{d}_M
- Forward calculation
- Possible distribution verification

$$\bar{d}_M = \bar{R} \bar{E}_N$$

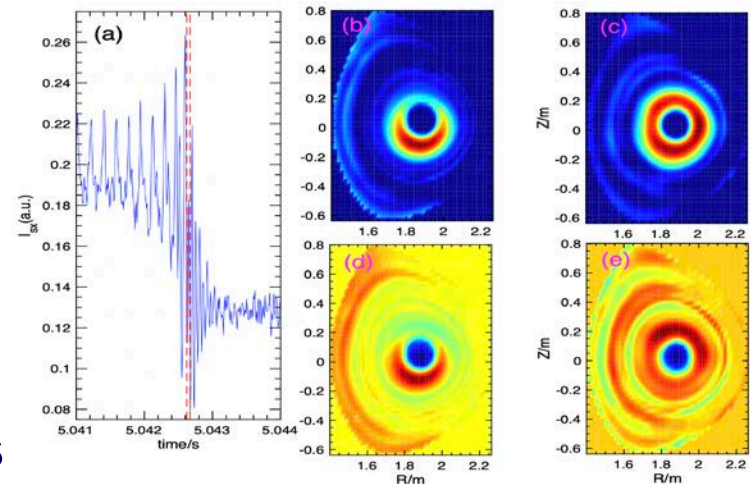
- **Inverse problem**

- From \bar{d}_M to \bar{E}_N
- Indirect method
- ill-posed problem, multi-solutions



possible distribution

measurements & calculations



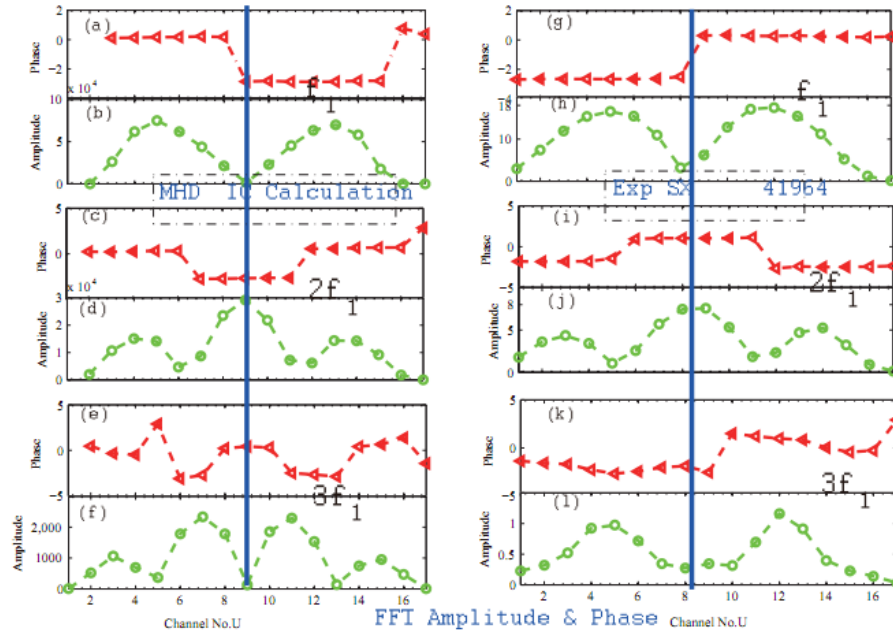
SXR reconstructions



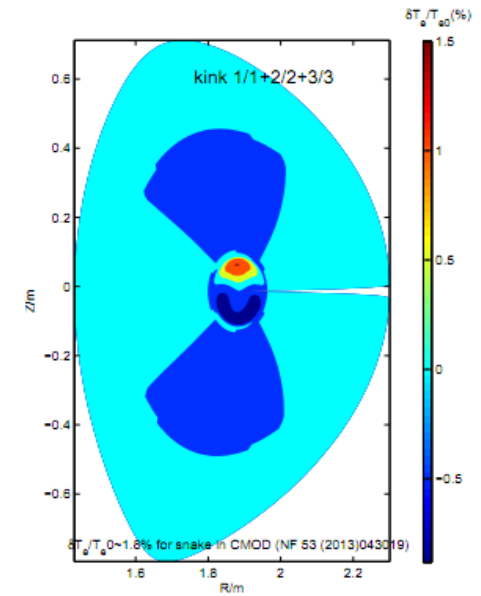
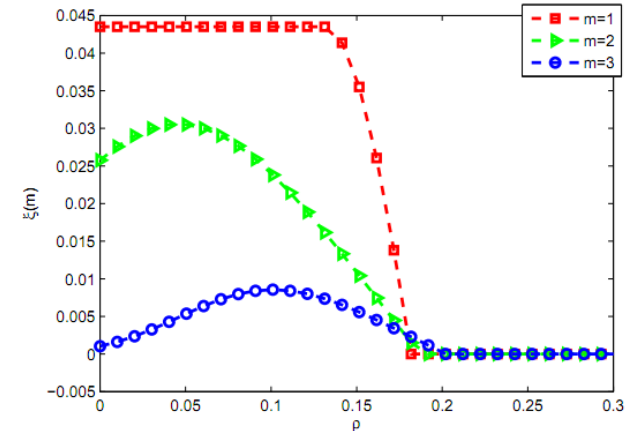
Forward method

Key issues

- Plenty prior information (predicted by codes)
- Plenty comparison of measurements and calculations (multi-arrays detection, perturbation amplitude and phase)



amplitude vs. phase



hypothetical distribution(1-D/2-D)



Outline

I. 2-D Tomographic reconstruction

II. Tomography methods on EAST

- Abel method
- Fourier-Bessel method (SXR)
- Constrained optimization method (divertor XUV)
- L-curve Tikhonov method (GEM)
- Gaussian progress method (SXR, HX and XUV)
- Neural network method (CNN, FCNN and VGGNet)

III. Applications

- MHD mode structure analysis (by SVD)
- Impurity density estimation

IV. Summary and Outlook



(1) Abel method

Abel model:

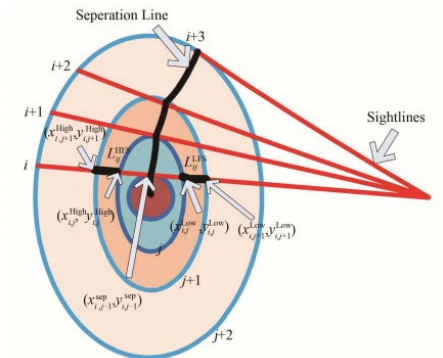
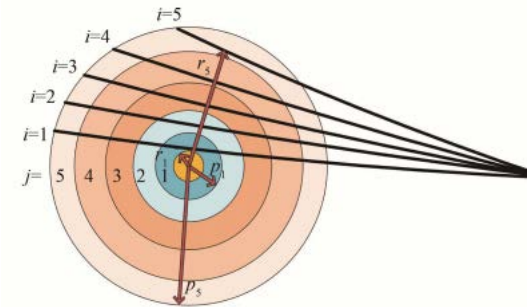
$$E_j = \sum_i L_{ij}^{-1} B_i$$

circular:

$$L_{ij} = \begin{cases} 2\sqrt{p_j^2 - r_i^2} & (p_j > r_i, i = j) \\ 2(\sqrt{p_j^2 - r_i^2} - \sqrt{p_{j-1}^2 - r_i^2}) & (p_j > r_i, i \neq j) \\ 0 & (p_j < r_i) \end{cases}$$

non-circular:

$$L_{ij} = \begin{cases} \sqrt{(x_{i,j}^{\text{High}} - x_{i,j-1}^{\text{High}})^2 + (y_{i,j}^{\text{High}} - y_{i,j-1}^{\text{High}})^2} + \\ \sqrt{(x_{i,j}^{\text{Low}} - x_{i,j-1}^{\text{Low}})^2 + (y_{i,j}^{\text{Low}} - y_{i,j-1}^{\text{Low}})^2} & (i < j) \\ \sqrt{(x_{i,j}^{\text{High}} - x_{i,j}^{\text{Low}})^2 + (y_{i,j}^{\text{High}} - y_{i,j}^{\text{Low}})^2} & (i = j) \\ 0 & (i > j) \end{cases}$$



Processes the 2-D problem to 1-D, too simple to applicate to SXR, XUV and HX complex tomography in Tokamak.



(2) Fourier-Bessel method (SXR)

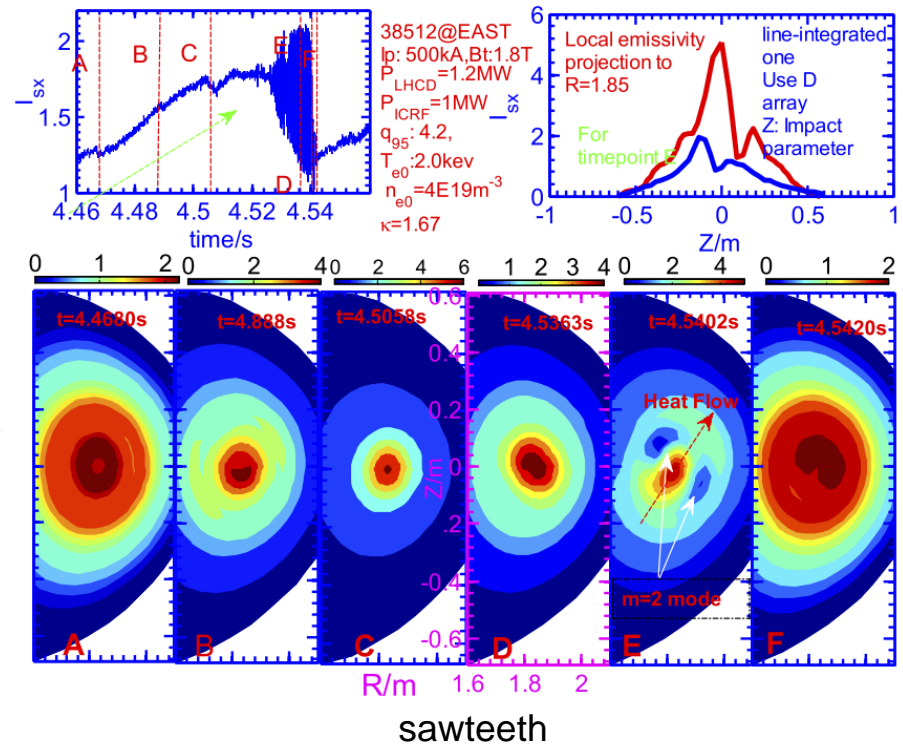
Angular Fourier expansion of emissivity:

$$g(r, \theta^*) = \sum_{m=0}^M [g_m^c(\rho) \cos(m\theta^*) + g_m^s(\rho) \sin(m\theta^*)]$$

Radial Bessel expansion of emissivity:

$$f = \sum_{m=0}^M \sum_{l=0}^L \int_L [a_{ml}^c(\rho) \cos(m\theta^*) + a_{ml}^s(\rho) \sin(m\theta^*)] J_m(\lambda_m^{l+1} \rho) dL$$

- LFCS as boundary (emissivity=0)
- Suitable for SXR (core SXR emissivity and core MHD perturbation reconstruction)
- Unsuitable for XUV
- Smooth reconstructions

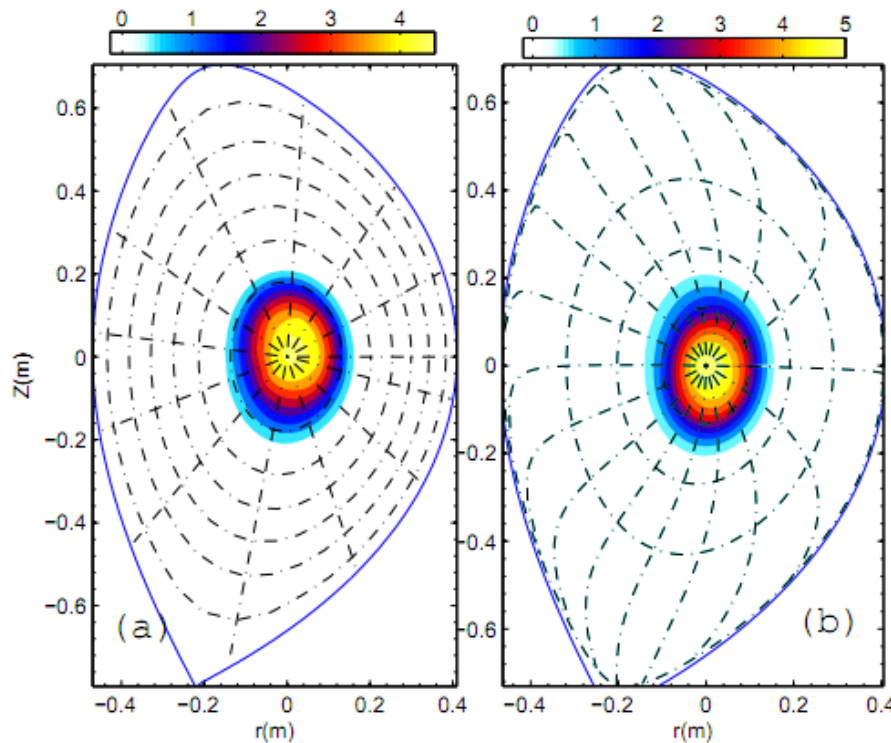


K. Chen, L. Xu[#], et al., *Rev. Sci. Instrum.* 87 (2016) 063504

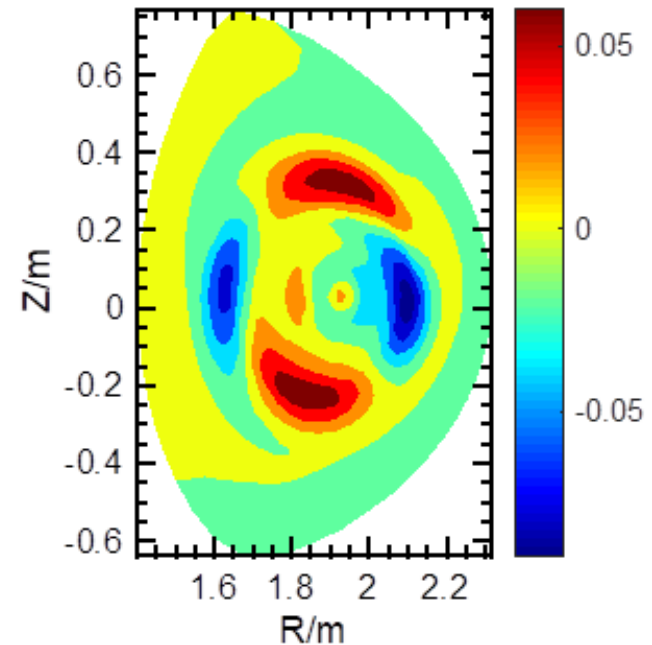


(2) Fourier-Bessel method (SXR)

- **Magnetic flux coordinates for non-circular configuration** (to characterize polar angle and radius accurately).
- **Assuming emissivity is a function of ψ .**
- **Suitable for reconstructing core SXR and peaking XUV emissivity.**



magnetic flux vs. Cartesian polar coordinates



mode $m=2$



(3) Constrained optimization method (divertor XUV)

Minimum problem:

$$\chi^2 = (Kg - f)^T W (Kg - f) = 0$$

Regular matrix:

$$\phi = \frac{1}{2} \chi^2 + \alpha \mathcal{R}$$

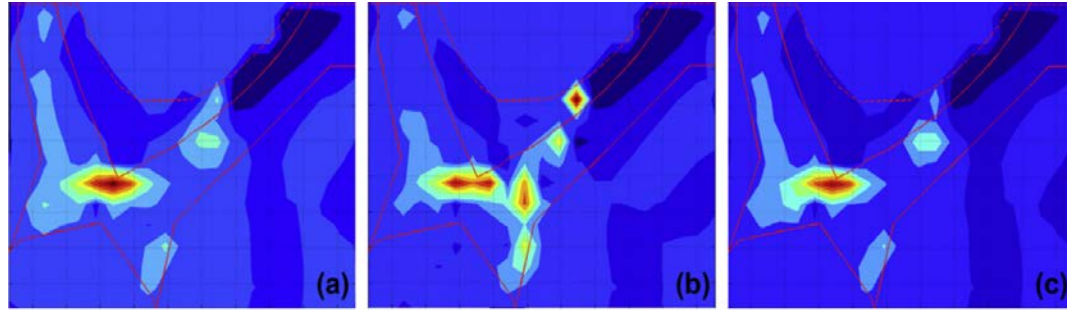
$$\begin{aligned} \mathcal{R}(\mathbf{g}) &= \iint \left\{ \nabla \cdot [\mathbf{D} \cdot \nabla g(x, y)] \right\}^2 dx dy \\ &= \iint \left[\nabla \cdot (n D_{\perp} n \cdot \nabla g(x, y) + t D_{\parallel} t \cdot \nabla g(x, y)) \right]^2 dx dy \end{aligned}$$

$$\begin{aligned} \mathbf{H} &= (C_x D_x + C_y D_y + C_{xx} D_{xx} + 2C_{xy} D_{xy} + C_{yy} D_{yy})^T F (C_x D_x \\ &\quad + C_y D_y + C_{xx} D_{xx} + 2C_{xy} D_{xy} + C_{yy} D_{yy}) \Delta x \Delta y + C_0 \end{aligned}$$

$$F_{ij}^{(n)} = \begin{cases} \left(\frac{\bar{g}^{(n)}}{g_j^{(n)}} \right)^{\beta} \delta_{ij} & , \quad g_j^{(n)} \geq \gamma \bar{g}^{(n)}, \quad n > 0 \\ \delta_{ij} & , \quad g_j^{(n)} < \gamma \bar{g}^{(n)}, \quad n > 0 \end{cases}$$

C: diagonal matrix **D:** matrix derivative

C₀: Constant matrix, to adjust the emissivity of a specific area



XUV reconstructions of divertor plasma during ELMs

Y. Duan, et al., *J. Nucl. Meter.*. 438 (2013) S228-S341

- **XUV radiation outside LFCS can be reconstructed (reconstructions will not be negative like the maximum entropy method).**
- **Regular matrix introduces two free parameters (complicated regular matrix)**
- **Equilibrium needed**
- **No large radial radiation gradient**



(4) L-curve Tikhonov method (GEM)

Introduce $\|\lambda C \varepsilon\|$:

$$(L^T L + \lambda C^T C) \varepsilon = L^T g$$

$$C_{i,j} = \begin{cases} -4 & (j = i) \\ 1 & (j = i \pm 1, j = i \pm nR) \\ 0 & \end{cases}$$

$$\rho^2 = \|L \varepsilon_\lambda - g\| \quad \eta^2 = \|C \varepsilon_\lambda\|$$

λ : free parameter C : positive definite matrix

ρ^2 : error caused by Positive definite matrix

η^2 : error caused by ill-posed problem

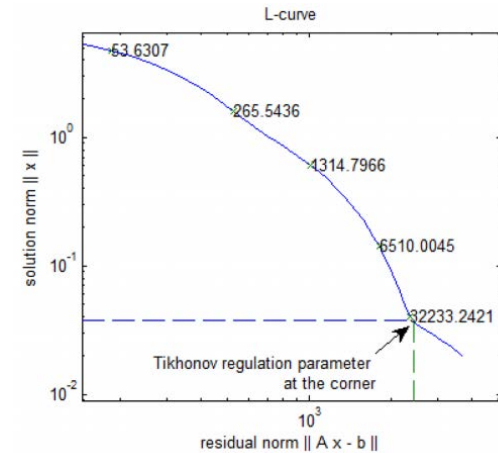
Positive definite term error: $\|Ax - b\|^2 = \lambda^4 \sum_{i=1}^n (\beta_i / (\gamma_i^2 + \lambda^2))^2$

Residual error: $\|x\|^2 = \sum_{i=1}^n (\gamma_i \beta_i / (\gamma_i^2 + \lambda^2))^2$.

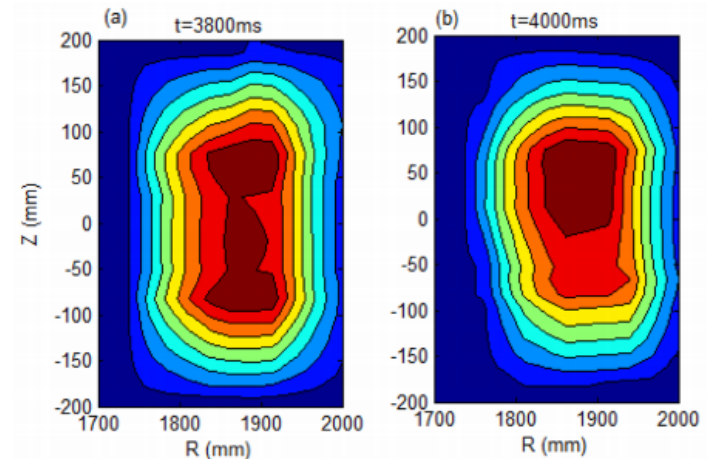
$$(L \cdot C^{-1}) = U \cdot \gamma \cdot V^T, \quad \beta = U^T \cdot I$$

(β and γ can be obtained by SVD)

- Simple positive definite matrix (no need for equilibrium)
- λ determined by L-curve technology
- Radial radiation symmetry assumed (mapping 3D measurements to 2D cross-section)



L-curve method to determine λ



2-D core Fe impurities (GEM)

H. Qu, et al., *Rev. Sci. Instrum.* 90 (2019) 093507



(5) Gaussian progress method (SXR, HX and XUV)

Bayesian inference:

$$p(\mathbf{E}_n | \mathbf{d}_m, \boldsymbol{\theta}) = \frac{p(\mathbf{d}_m | \mathbf{E}_n, \boldsymbol{\theta}) \cdot p(\mathbf{E}_n | \boldsymbol{\theta})}{p(\mathbf{d}_m | \boldsymbol{\theta})} \sim p(\mathbf{d}_m | \mathbf{E}_n, \boldsymbol{\theta}) \cdot p(\mathbf{E}_n | \boldsymbol{\theta})$$

posterior probability
likelihood probability
prior probability

Gaussian Process modelling:

prior probability $p(\mathbf{E}_n | \boldsymbol{\theta}) = \frac{1}{(2\pi)^{\frac{n}{2}} |\boldsymbol{\Sigma}_E^{prior}|^{\frac{1}{2}}} \exp \left[-\frac{1}{2} (\mathbf{E}_n - \boldsymbol{\mu}_E^{prior})^T \boldsymbol{\Sigma}_E^{prior^{-1}} (\mathbf{E}_n - \boldsymbol{\mu}_E^{prior}) \right]$

likelihood probability $p(\mathbf{d}_m | \mathbf{E}_n, \boldsymbol{\theta}) = \frac{1}{(2\pi)^{\frac{m}{2}} |\boldsymbol{\Sigma}_d|^{\frac{1}{2}}} \exp \left[-\frac{1}{2} (\mathbf{R} \cdot \mathbf{E}_n - \mathbf{d}_m)^T \boldsymbol{\Sigma}_d^{-1} (\mathbf{R} \cdot \mathbf{E}_n - \mathbf{d}_m) \right]$

posterior probability $p(\mathbf{E}_n | \mathbf{d}_m, \boldsymbol{\theta}) \sim \exp \left[\begin{array}{c} -\frac{1}{2} (\mathbf{R} \cdot \mathbf{E}_n - \mathbf{d}_m)^T \boldsymbol{\Sigma}_d^{-1} (\mathbf{R} \cdot \mathbf{E}_n - \mathbf{d}_m) \\ -\frac{1}{2} (\mathbf{E}_n - \boldsymbol{\mu}_E^{prior})^T \boldsymbol{\Sigma}_E^{prior^{-1}} (\mathbf{E}_n - \boldsymbol{\mu}_E^{prior}) \end{array} \right]$

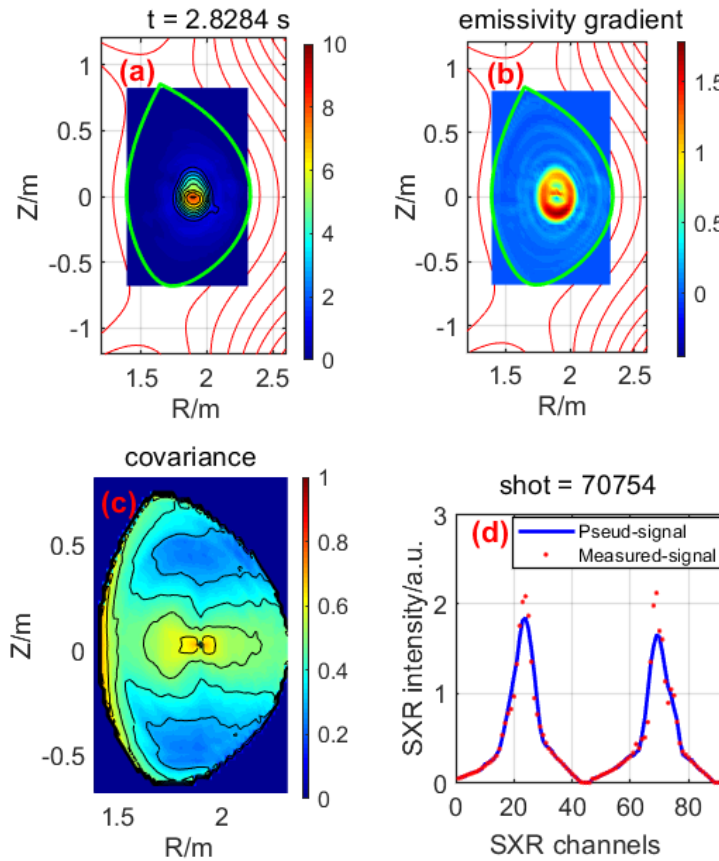
Uncertainty: $\boldsymbol{\Sigma}_E^{post} = \left(\mathbf{R}^T \boldsymbol{\Sigma}_d \mathbf{R} + \boldsymbol{\Sigma}_E^{prior^{-1}} \right)^{-1}$ (covariance matrix of posterior)

Emissivity inferred: $\boldsymbol{\mu}_E^{post} = \boldsymbol{\mu}_E^{prior} + \left(\mathbf{R}^T \boldsymbol{\Sigma}_d \mathbf{R} + \boldsymbol{\Sigma}_E^{prior^{-1}} \right)^{-1} \mathbf{R}^T \boldsymbol{\Sigma}_d^{-1} (\mathbf{d}_m - \mathbf{R} \cdot \boldsymbol{\mu}_E^{prior})$
(mean vector of posterior)



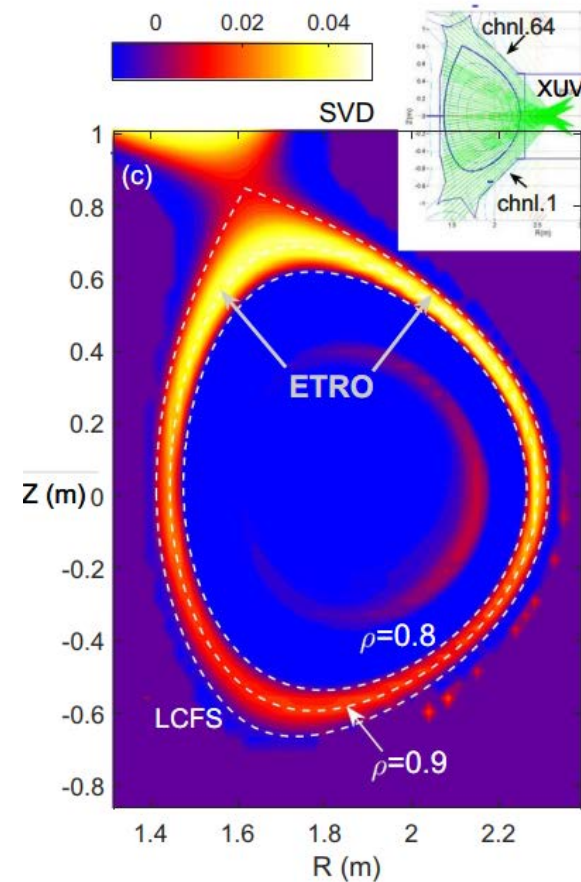
(5) Gaussian progress method (SXR, HX and XUV)

- Uncertainty analysis & potential to real-time application



MHD-SXR-GPT reconstruction

Y. Chao, L. Xu[#], et al., *Chin. Phys. B* 29 (2020) 095201



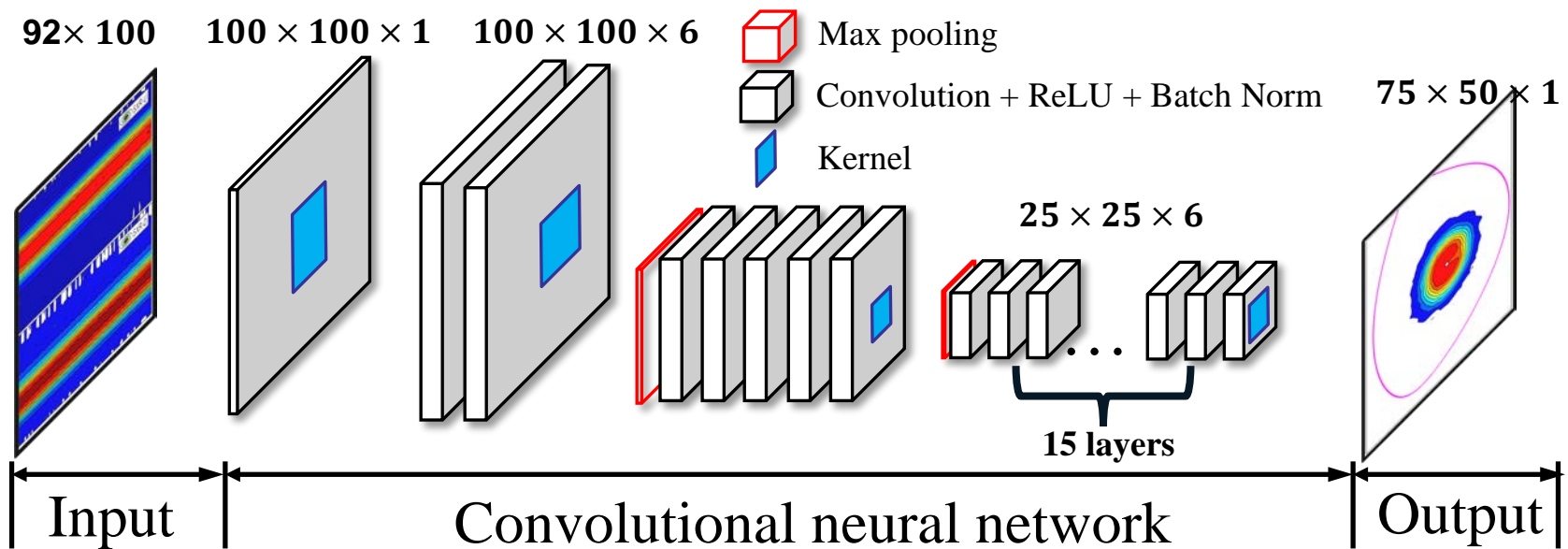
ETRO-XUV-GPT reconstruction

A. D. Liu et al., *Nucl. Fusion* 60 (2020) 126016



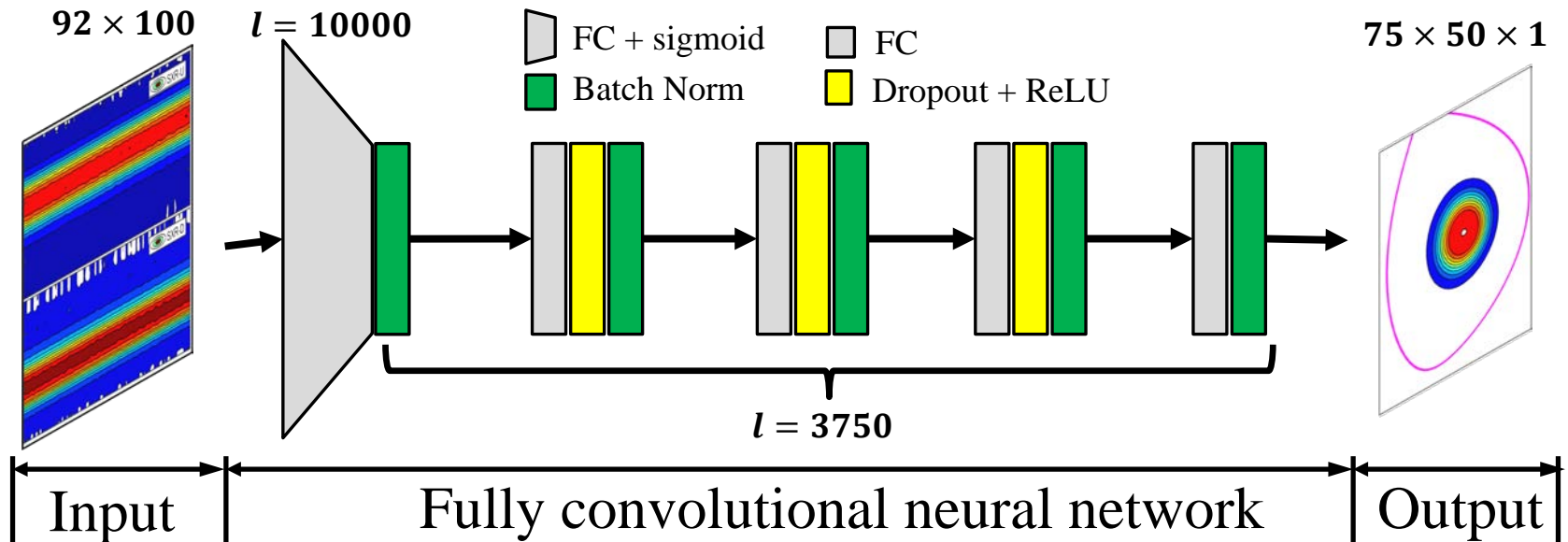
(6) Convolutional Neural Network (CNN)

- CNN only consists of convolutional layers
- The number of parameters is $O(l)$ (l is the size of data)
- First three layers: (1,1), (7,7), (7,7) others: (3,3) kernels



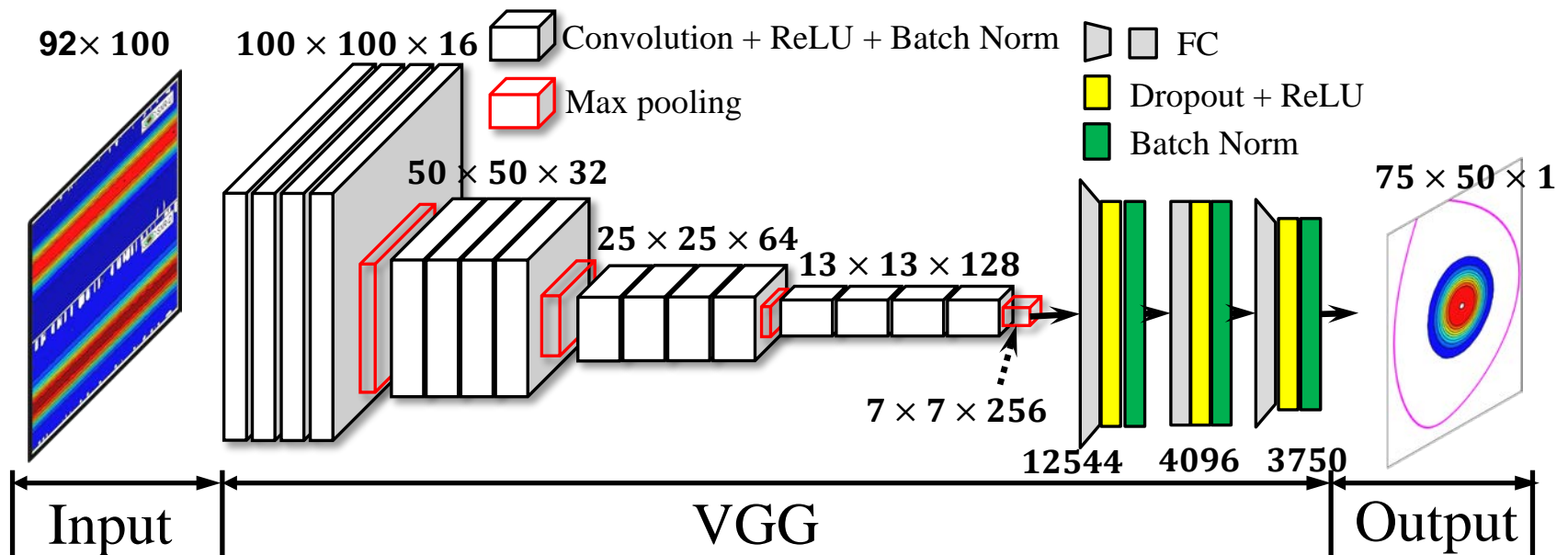
(6) Fully Convolutional Neural Network (FCNN)

- FCNN consists of fully convolutional (FC) layers
- The number of parameters is $O(l^2)$ (l is the size of data)
- Dropout layers are added after FC for optimization



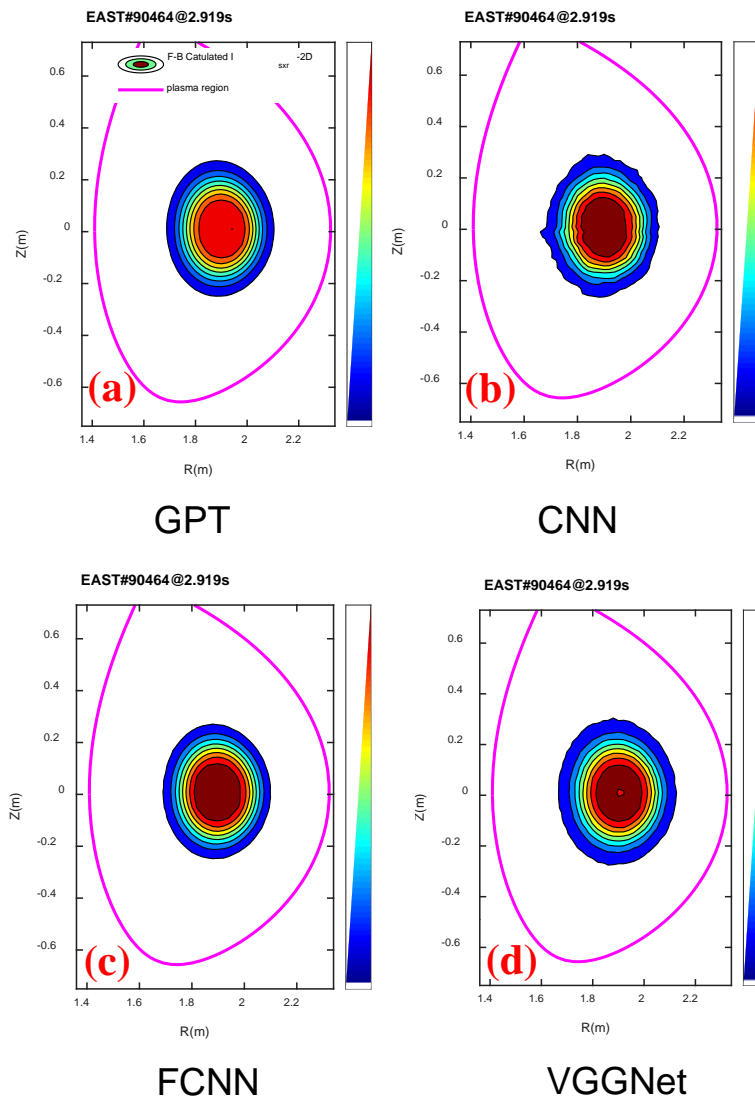
(6) Visual Geometry Group Net (VGGNet)

- VGGNet consists of FC and convolutional layers
- For convolution layers: (3,3) kernel (every 4 layers, pooling halve and the channel double)
- For FC layers, Dropout layers are added for optimization



(6) Reconstruction results

- **Input layer: 92 SXR LOS measurements** (with interaction dimension expansion)
- $ReLU = \begin{cases} x, & x > 0 \\ 0, & x \leq 0 \end{cases}$ (Rectified linear unit (ReLU))
- **Output layer: 75×50 matrix** (with ReLU activation), SXR emissivity map



	CNN	FCNN	VGGNet	GPT
Tests	1000	1000	1000	\
Averaged Maximum Error	29.3%	57.03%	46.96%	\
RMSD	1.49 $\times 10^{-4}$	4.086 $\times 10^{-5}$	2.784 $\times 10^{-5}$	\
Execution time	3 ms	25.5 ms	34.9ms	$\geq 47s$

Outline

I. 2-D Tomographic reconstruction

II. Tomography methods on EAST

- Abel method
- Fourier-Bessel method (SXR)
- Constrained optimization method (divertor XUV)
- L-curve Tikhonov method (GEM)
- Gaussian progress method (SXR, HX and XUV)
- Neural network method (CNN, FCNN and VGGNet)

III. Applications

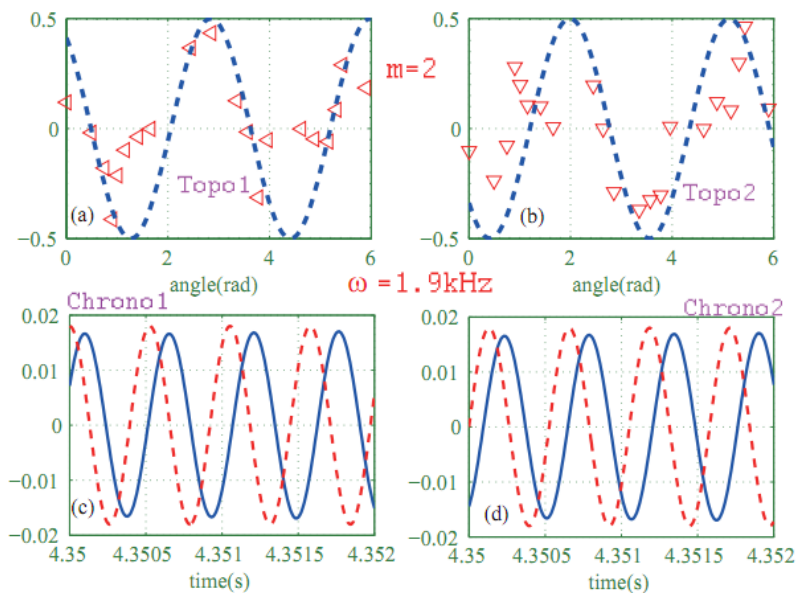
- MHD mode structure analysis (by SVD)
- Impurity density estimation

IV. Summary and Outlook

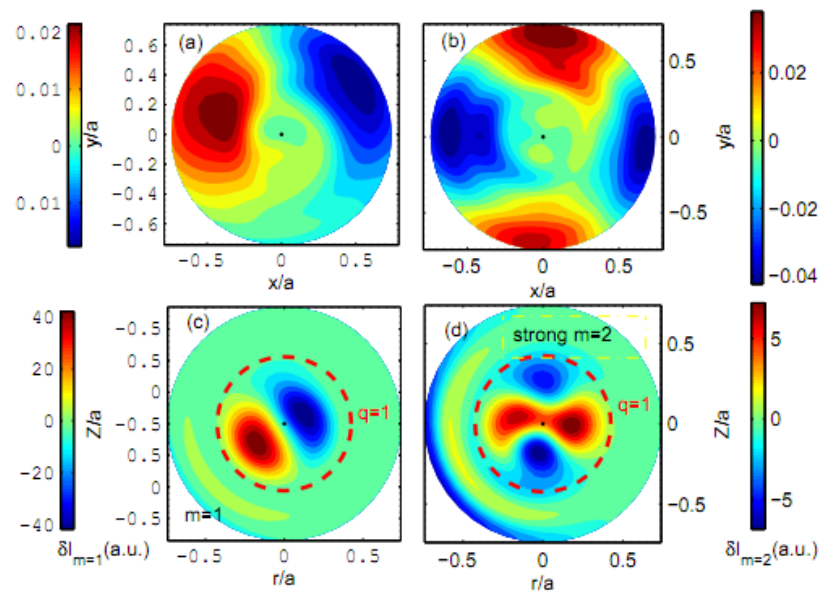


MHD mode structure analysis (by SVD)

- $A_{n \times p} = U_{n \times n} \cdot S_{n \times p} \cdot V_{p \times p}^T$ ($U_{n \times n}$ and $V_{p \times p}$ are orthogonal, $S_{n \times p}$ represents the weight of each topo/chrono)
- Applications: blurred image recognition/restoration, signal denoising and MHD mode structure analysis.



spatial-temporal signals decomposed by SVD



MHD coupling components decomposed by SVD

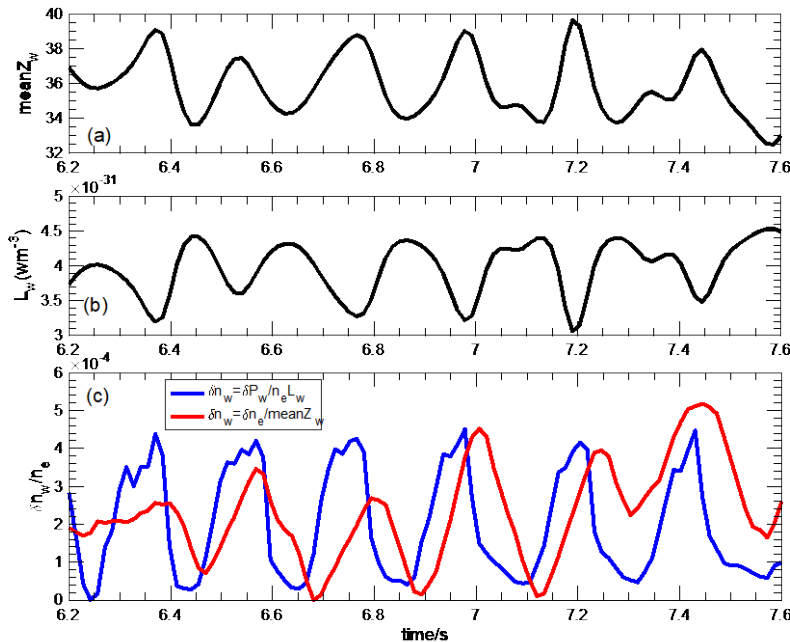
L. Xu, et al., *Chin. Phys. B* 21 (2012) 055208



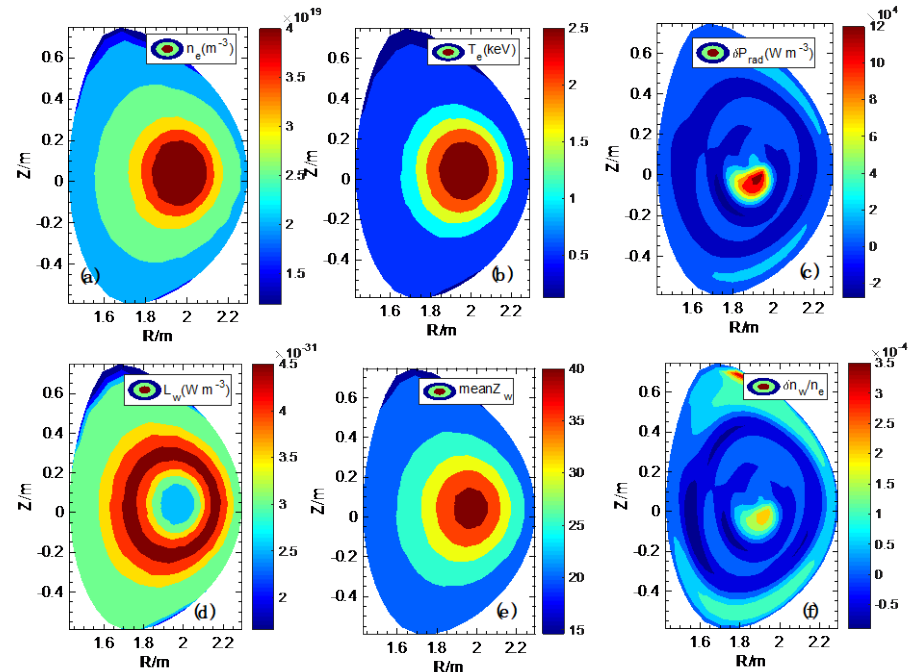
Impurity density estimation

- $\Delta n_w = \Delta n_e / Z_w$
- $\Delta n_w = \Delta p_w / (L_w n_e)$

Δn_e measured by point
 Δp_w reconstructed from XUV
 Z_w and L_w from ADAS



impurity density evolution



2-D impurity density distribution



Outline

I. 2-D Tomographic reconstruction

II. Tomography methods on EAST

- Abel method
- Fourier-Bessel method (SXR)
- Constrained optimization method (divertor XUV)
- L-curve Tikhonov method (GEM)
- Gaussian progress method (SXR, HX and XUV)
- Neural network method (CNN, FCNN and VGGNet)

III. Applications

- MHD mode structure analysis (by SVD)
- Impurity density estimation

IV. Summary and Outlook



Summary

- A variety tomography methods have been developed on EAST (including Fourier-Bessel, constrained optimization, L-curve Tikhonov, Gaussian progress and neural network methods). The pros&cons and the application scope of these methods are analyzed.
- Developed MHD mode structure analysis method based on SVD, combined with tomography can recognize complicated MHD. The impurity density can be obtained by combining XUV and SXR reconstructions.
- The GPT method, which runs fast with uncertainty analysis, has been implemented to HX, SXR and XUV on EAST, supporting MHD and transport research.



Outlook

- Implement the GPT method to more diagnostics (such as neutron imaging diagnostic), and further optimize it for the SXR real-time tomography.
- Realize real-time core heavy impurity density estimation to support EAST H-mode long-pulse operation.
- Develop new tomography method for SXR and XUV (based on machine training and big data analytics, such as neural networks), to avoid the large radial XUV radiation gradient of reconstructions.



Thank you for the attention!

